Scatterometry for *in situ* measurement of pattern reflow in nanoimprinted polymers

Heather J. Patrick,[1,2,a)] Thomas A. Germer,[1] Yifu Ding,[1,3] Hyun Wook Ro,[1] Lee J. Richter,[1] and Christopher L. Soles[1]
[1]*National Institute of Standards and Technology, Gaithersburg, Maryland 20899, USA*
[2]*KT Consulting, Inc., Antioch, California 94509, USA*
[3]*Department of Mechanical Engineering, University of Colorado at Boulder, Boulder, Colorado 80309, USA*

(Received 18 November 2008; accepted 20 November 2008; published online 9 December 2008)

We use optical scatterometry to extract the time evolution of the profile of nanoimprinted lines in low and high molecular mass polymer gratings during reflow at the glass transition temperature. The data are obtained continuously during the anneal using a spectroscopic ellipsometer and analyzed using a rigorous-coupled-wave model. We show excellent agreement of scatterometry results with *ex situ* measurements of line height by atomic force microscopy and specular x-ray reflectivity. The *in situ* scatterometry results reveal differences in the shape evolution of the grating lines indiscernible by other methods. © *2008 American Institute of Physics*. [DOI: 10.1063/1.3046117]

Nanoimprint lithography (NIL), in which features on a prepatterned mold are transferred directly into a polymer material, is a rapidly maturing alternative to optical lithography for nanoscale fabrication. The thermal embossing form of NIL can also be used to directly pattern functional polymers, e.g., those that have semiconducting, piezoelectric, or insulating properties, without first creating the pattern in a sacrificial photoresist. The way that the imprint process affects the patterned material can critically impact the performance of the directly patterned structure. Recent studies have shown that measuring the shape evolution (reflow) of nanoimprinted lines during thermal annealing can provide important information about the levels of residual stress induced by NIL processing, the roles of polymer viscosity and rheology in creating those stresses, and their ultimate impact on the stability of patterns of different molecular masses.[1–4]

In this work, we use optical scatterometry to provide *in situ*, nondestructive measurements of the reflow of thermal embossed NIL line gratings in polystyrene. In contrast with the more widely used pattern characterization techniques of cross-sectional scanning electron microscopy (SEM) and atomic force microscopy (AFM), which are time consuming, require sectioning of the sample (in the case of SEM), and typically require multiple samples quenched following annealing for different times to build up a complete picture of the reflow, scatterometry provides a continuous real-time annealing record from a single sample. We will show that scatterometry line heights are in excellent agreement with values obtained *ex situ* using AFM and specular x-ray reflectivity (SXR), another line profiling technique recently used for nanoimprinted films.[5] Scatterometry also provides a table-top alternative to line profiling by critical dimension small-angle x-ray scattering (CD-SAXS),[6] which requires an intense, synchrotron-based x-ray source. While scatterometry has previously been applied to the study of nanoimprinted polymers,[3,4,7] the current work is the first successful demonstration of its use for quantifying line profiles *in situ* during reflow and provides new insight into the profile evolution of gratings with high and low molecular masses.

Gratings were prepared from thin films of low-polydispersity-index polystyrene (PS) with molar masses of 18.1 and 1571 kg mol^{-1}, referred to here as PS18k and PS1570k, respectively. PS films ~300 nm thick on Si wafer substrates were imprinted on a Nanonex NX-2000 imprinter[8] using a silicon oxide imprinting mold that had gratings with a pitch of ~420 nm, height of ~360 nm, and a line to space ratio of 1:1.6. The area of each grating was 5×20 mm^2. The PS films were imprinted under vacuum at 40 °C above the glass transition temperature (T_g) of the bulk polymer, and then cooled to 55 °C before releasing the mold. The resulting imprinted patterns consisted of 420 nm pitch grating lines over a uniform residual layer of PS. The imprinted wafer was divided into individual 5×20 or 5×10 mm^2 sample chips. Additional details of the imprinting procedure can be found in Ref. 1.

We used spectroscopic ellipsometry (SE) to characterize the imprinted PS gratings and the as-spun PS films. The ellipsometric parameters[9] α and β were measured at 616 points over wavelengths ranging from 335 to 1700 nm using a rotating-compensator variable-angle spectroscopic ellipsometer. Figure 1 shows typical SE spectra. Although the ellipsometer's wavelength range extends to 190 nm with an ultraviolet (uv) lamp, the uv lamp was turned off for the current study because it visibly damaged gratings in preliminary measurements. The size of the measurement spot on the sample was approximately 0.3×0.6 mm^2. The incident angle was fixed at 60° from normal, and the chip was aligned with the grating lines perpendicular to the plane of incidence.

To anneal the gratings, a hot stage mounted on the ellipsometer was preheated to the T_g of the PS (100 °C for PS18k or 106 °C for PS1570k), and an individual chip was placed on the preheated stage. Following a 1.5 min delay, required to verify chip alignment, SE data were acquired every 12 s over 2 h. In addition to the *in situ* annealing, a number of other PS18k and PS1570k chips were annealed for a series of shorter times for use in the *ex situ* measurements.

a)Electronic mail: heather.patrick@nist.gov.

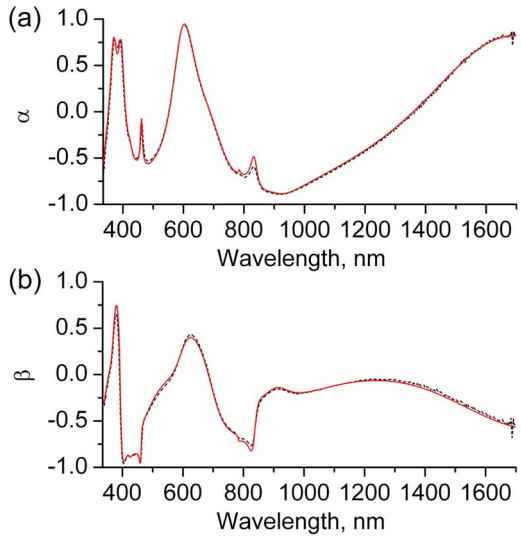

FIG. 1. (Color online) SE (a) α and (b) β spectra (black dashed curves) and scatterometry model fits (red solid curves) measured during annealing of a PS18k grating at $T_g=100$ °C. The measurement was made at 1.7 min into the anneal, and the line profile corresponding to the fit is the tallest green solid line profile in Fig. 3(b).

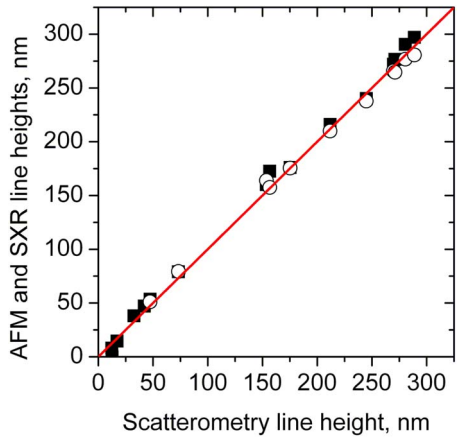

FIG. 2. (Color online) Comparison of line height measured by scatterometry with line height measured by AFM (solid squares) and SXR (open circles). The line $y=x$ is also shown.

The SE data were modeled using rigorous-coupled-wave (RCW) analysis.[10–12] We developed a parametrized model for the shape of the lines in the grating using *a priori* knowledge of the probable line structure, then calculated theoretical SE spectra for different combinations of the line parameters, a technique often referred to as scatterometry.[13] An accurate model for the line profile is essential for achieving good agreement between measured and theoretical spectra. Here, the profile model includes a residual PS layer and grating lines that can vary in cross section from trapezoidal to nearly sinusoidal by convolving a trapezoid with a Gaussian. The profile parameters are the top and bottom linewidths, the line height of the trapezoid, the residual layer thickness, the pitch, and the width of the Gaussian.

We performed nonlinear weighted least-squares fits of the SE spectra to the RCW model using a Levenberg–Marquardt algorithm,[14] letting all of the profile parameters vary except pitch, which was fixed at 419.8 nm, as determined from a laser diffractometer. The silicon substrate optical constants were fixed at values taken from the literature.[15] The optical constants for PS18k and PS1570k were fixed at values determined from SE of thin films of the respective materials;[9] separate optical dispersions were measured from hot (at T_g) and room temperature films. For the RCW calculations, the modulated portion of the gratings was divided into $k=20$ layers, and the Floquet expansions of the fields were truncated at $M=5$. Initial fits to the SE spectra for the as-imprinted grating samples were made using libraries of trapezoidal profiles with minimal smoothing. After the best fit profiles were found, the first SE spectra taken during annealing were fit using the parameters from the as-imprinted gratings as initial values. Subsequent spectra were fit starting with parameters from the previous spectrum.

Figure 1 shows an example SE data set, taken during annealing of a PS18k grating at $T_g=100$ °C, and the best fit to the data using the scatterometry model. The fit quality seen here is typical of that seen for early anneal time SE data, with the model reproducing all of the significant features in the spectrum, but with some small discrepancies in the sharper features around 480 and 800 nm that are associated with the grating modulation. Fit qualities improved at later anneal times. The positions of the broad features in the α spectrum, such as the peak near 600 nm, are determined in part by the residual layer thickness. An advantage of scatterometry profiling, in addition to its speed, is that, as with SXR, but unlike AFM, the residual layer thicknesses can be extracted along with the grating line profiles.

Because the evolution of grating height during reflow has been shown to provide crucial insight into polymer rheology,[1–3] we compared scatterometry measurements of line height with results obtained by SXR and AFM as an important first step in validating the scatterometry method. As SXR and AFM could not be done *in situ*, we used the set of *ex situ* samples for these measurements. The agreement between scatterometry and the other techniques, shown in Fig. 2, is striking. The mean and standard deviation of the difference between scatterometry and SXR heights were 0.9 and 5.8 nm, respectively, and between scatterometry and AFM, −3.1 and 6.8 nm, respectively. Fewer SXR measurements are shown because samples with line heights of less than 50 nm did not give sufficient reflectance for successful SXR modeling. A full uncertainty analysis was not performed for each method, and this comparison does not address the absolute accuracy of the respective methods. While agreement between the techniques is very good, the observed variance may arise in part from sample nonuniformity. The SXR measurement covers the full chip, the AFM, just a few lines, and the ellipsometer, a millimeter-scale area.

We now turn to the *in situ* annealing results. Figure 3(a) shows the measured line height versus time for PS18k and PS1570k gratings, which indicates very different reflow mechanisms for gratings of different molecular masses. The PS18k height decay is close to exponential with time, as expected for a simple liquid with surface-tension-dominated viscous flow.[1] The PS1570k height shows a fast early relaxation that has been attributed to an elastic recovery of residual stress locked into the more highly entangled, longer chain polymers during imprinting,[1] followed by a plateau with a much slower decay rate. We are not restricted to looking at height, however, but are also able to obtain the full profile of the grating lines. Figure 3(b) shows the line profiles of the PS18k and PS1570k gratings at the first point measured during annealing, then at ~175 nm heights and

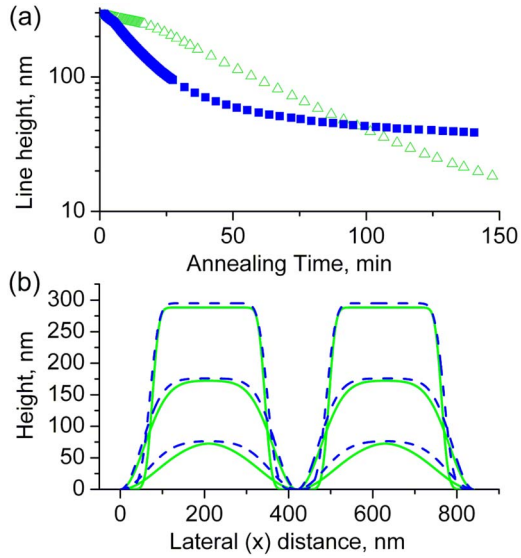

FIG. 3. (Color online) (a) Line height vs time measured by scatterometry for a PS18k grating (open green triangles) during annealing at $T_g = 100\ ^\circ\mathrm{C}$ and a PS1570k grating (closed blue squares) during annealing at $T_g = 106\ ^\circ\mathrm{C}$. (b) Line profiles of the PS18k grating (green solid curves) and the PS1570k grating (blue dashed curves) for three similar grating heights. The underlying residual PS layer is not shown.

~75 nm heights. While the profiles are initially similar, the PS1570k grating holds a more trapezoidal shape as the grating decays. In contrast, at 75 nm height, the PS18k pattern has decayed to a nearly sinusoidal profile. The PS1570k line profiles support the hypothesis in Ref. 1 that elastic recovery, rather than a surface tension induced "shear thinning" effect, dominates the PS1570k pattern decay. The surface-tension-induced Laplace pressure at the corners is larger than that associated with the overall line profile, suggesting more severe shear thinning at the corners. Therefore, if the overall faster pattern decay rate of PS1570k was caused by shear thinning, the corner rounding rate should also be higher in PS1570k, opposite to the experimental observations.

As a check on the validity of the line profile model, we evaluated the total volume of polymer [including polymer in the residual layer, not shown in Fig. 3(b)] in the line profiles associated with every data point in Fig. 3(a). The pattern volume was indeed found to be conserved, with peak-to-peak variation of 0.6% for both the PS1570k and PS18k gratings. Nearly all of the volume variation was observed early in the anneal, when we obtain relatively poorer fits to the profile model. The Gaussian-convolved trapezoid selected for this initial study restricts the smoothening to be the same at the top and bottom corners, an assumption which may need to be revisited for early stage annealing in future profile model development. We also anticipate further profile comparisons with *ex situ* techniques such as SXR, and with theoretical predictions of polymer rheology, in follow-up studies.

In summary, we have demonstrated that scatterometry provides a powerful technique for quantifying the reflow of line gratings in nanoimprinted polymers *in situ* during annealing. The results of scatterometry for line height are in excellent agreement with *ex situ* techniques, and scatterometry has the advantages of providing the thickness of the residual layer, which AFM cannot, and of successfully profiling gratings with modulations less than 50 nm, which is difficult for SXR. The *in situ* line profiles obtained from scatterometry reveal clear shape differences in the decay of gratings with different molecular masses, and we anticipate the successful use of scatterometry in elucidating the detailed mechanisms of pattern stability in NIL.

[1] Y. Ding, H. W. Ro, K. J. Alvine, B. C. Okerberg, J. Zhou, J. F. Douglas, A. Karim, and C. L. Soles, Adv. Funct. Mater. **18**, 1854 (2008).
[2] Y. Ding, H. W. Ro, T. A. Germer, J. F. Douglas, B. C. Okerberg, A. Karim, and C. L. Soles, ACS Nano **1**, 84 (2007).
[3] T. Leveder, S. Landis, L. Davoust, S. Soulan, J.-H. Tortai, and N. Chaix, J. Vac. Sci. Technol. B **25**, 2365 (2007).
[4] R. M. Al-Assaad, L. Tao, and W. Hu, J. Micro/Nanolith. MEMS MOEMS **7**, 013008 (2008).
[5] H.-J. Lee, C. L. Soles, H. W. Ro, R. L. Jones, E. K. Lin, and W. Wu, Appl. Phys. Lett. **87**, 263111 (2005).
[6] R. L. Jones, T. Hu, C. L. Soles, E. K. Lin, R. M. Reano, S. W. Pang, and D. M. Casa, Nano Lett. **6**, 1723 (2006).
[7] D. Fuard, C. Perret, V. Farys, C. Gourgon, and P. Schiavone, J. Vac. Sci. Technol. B **23**, 3069 (2005).
[8] Certain commercial materials and equipment are identified in order to adequately specify the experimental procedure. Such identification does not imply recommendation by the National Institute of Standards and Technology.
[9] H. G. Tompkins, *A User's Guide to Ellipsometry* (Dover, Mineola, NY, 1993).
[10] M. G. Moharam, E. B. Grann, D. A. Pommet, and T. K. Gaylord, J. Opt. Soc. Am. A **12**, 1068 (1995).
[11] M. G. Moharam, D. A. Pommet, E. B. Grann, and T. K. Gaylord, J. Opt. Soc. Am. A **12**, 1077 (1995).
[12] L. Li, J. Opt. Soc. Am. A **13**, 1870 (1996).
[13] C. J. Raymond, in *Handbook of Silicon Semiconductor Metrology*, edited by A. C. Diebold (Dekker, New York, 2001), pp. 477–514.
[14] W. H. Press, S. A. Teukolsky, W. T. Vetterling, and B. P. Flannery, *Numerical Recipes in C*, 2nd ed. (Cambridge University Press, Cambridge, 1992).
[15] C. M. Herzinger, B. Johs, W. A. McGahan, J. A. Woolam, and W. Paulson, J. Appl. Phys. **83**, 3323 (1998).